GEOPHYSICAL RESEARCH LETTERS, VOL. 23, NO. 7, PAGES 745-748, APRIL 1, 1996

Detection of biomass burning smoke from TOMS measurements

N.C. Hsu[1], J.R. Herman[2], P.K. Bhartia[2], C.J. Seftor[1],O. Torres[1],
A.M. Thompson[2], J.F. Gleason[2], T.F. Eck[1], and B.N. Holben[3]

Abstract. A 14.5 year gridded data set of tropospheric absorbing aerosol index was derived from the Nimbus-7 Total Ozone Mapping Spectrometer (TOMS) reflectivity difference between 340 and 380 nm channels. Based upon radiative transfer calculations, the reflectivity anomaly between these two UV wavelength channels is very sensitive to smoke and soot aerosols from biomass burning and forest fires, volcanic ash clouds as well as desert mineral dust. We demonstrate the ability of the TOMS instrument to detect and track smoke and soot aerosols generated by biomass burning in South America. TOMS data can clearly distinguish between absorbing particles (smoke and dust) and non-absorbing aerosols (clouds and haze). For South American fires, comparisons of TOMS data are consistent with the limited amount of ground-based observations (Porto Nacional, Brazil) and show generally good agreement with other satellite imagery. TOMS data shows large-scale transport of smoke particulates generated by the burning fires in the South America, which subsequentially advects smoke aerosols as far as the Atlantic Ocean east of Uruguay.

Introduction

The effect of scattering and absorption by tropospheric aerosols in the Earth's radiative budget has gained increasing attention. Based on theoretical model calculations [*Westphal et al.*, 1989; *Robock*, 1988], smoke generated from forest fires could significantly change local temperatures near the surface and in the mid-troposphere. Haywood and Shine [1995] have also demonstrated, using a radiation model, that the effect of anthropogenic carbonaceous soot within the troposphere could play an important role in the clear sky planetary radiation budget. However, detailed understanding of the impact of tropospheric aerosols on regional and global climate, and thus on the greenhouse effect was still very poor because of the lack of the global tropospheric aerosol measurements.

Since the size of smoke particles from the fires is close to the visible wavelength, the smoke plumes generated by biomass burnings and forest fires have been effectively detected by the visible and near-IR channels of AVHRR (Advanced Very High Resolution Radiometer) and GOES (Geostationary Operational Environmental Satellite System) [Matson and Holben, 1987; Kaufman et al., 1992; Prins and Menzel, 1992]. However, separation of the clouds and smoke in the visible wavelength is time consuming and can not be easily done for operational use. Also the separation of the signal in the smoke from that of background terrestrial environments sometime can be difficult [Robinson, 1991].

A new absorbing aerosol index is discussed based on the reflectivity difference between the Version 7 reprocessed TOMS (Total Ozone Mapping Spectrometer) 340 nm and 380 nm channel data. TOMS reflectivity is obtained by removing the Rayleigh scattering component from the measured radiance-irradiance ratios for each wavelength channel not sensitive to ozone absorption (331 nm, 340 nm, 360 nm, and 380 nm). The resulting quantities contain information on clouds, surface reflectivity, and atmospheric aerosol scattering and absorption. When absorbing aerosols are present, the reflectivity is overcorrected for multiple Rayleigh scattering. The error is larger at shorter wavelengths. This results in a reflectivity difference , $R_{340} - R_{380} < 0$, that is a measure of the amount of absorbing aerosol in an atmosphere bounded by a wavelength independent lambertian reflecting surface.

Radiative transfer model simulations confirm that reflectivity differences between 340 and 380 nm wavelength are very sensitive to UV-absorbing aerosols in the stratosphere and troposphere, and weakly sensitive to non-absorbing aerosols in the lower troposphere. In this paper, we will demonstrate the ability of TOMS measurements to detect smoke from biomass burning, and other tropospheric absorbing particulates.

Biomass Burning in South America

Plate 1a shows the distribution of UV-absorbing aerosols derived from the TOMS measurements on August 18, 1987. These features are clearly distinguished from possible data artifacts (e.g., ocean sunglint) by observing their seasonal dependence and by constructing movies from TOMS daily observations. The seasonal dependence shows a total absence of the absorbing features when ground based observations (e.g., during the rainy season) indicate that there was no dust or burning. The movies show the temporal development and geographical spread following the prevailing winds.

In Plate 1a, TOMS detected a massive plume of desert dust stretched from the Sahara to the Atlantic Ocean that eventually extends over Cuba. Also, over the African continent and the south Atlantic Ocean near the equator, some smoke cloud was clearly visible on the TOMS map, which coincides with known times and locations of biomass burning in Africa [Cros et al.,1991; Connors et al., 1991]. In South America, a predominant feature was a large, roughly circular concentration of smoke centered at approximately 10°S and 55°W. Smoke remnants from earlier days were also observed near the coastal region in the Atlantic Ocean and west of the Andes.

[1] Hughes STX, 7701 Greenbelt Road, Greenbelt, Maryland
[2] Code 916, NASA/Goddard Space Flight Center, Maryland
[3] Code 923, NASA/Goddard Space Flight Center, Maryland

Paper number 96GL00455
0094-8534/96/96GL-00455$03.00

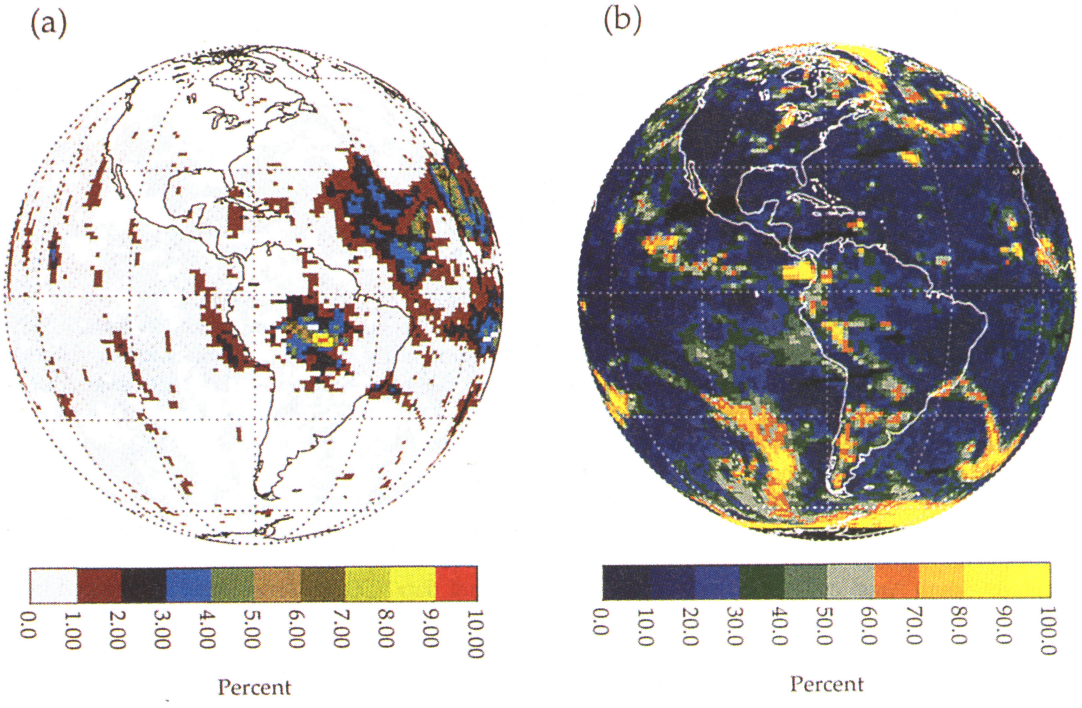

Plate 1. a) The map of TOMS reflectivity difference (R_{380}-R_{340}) over S. America and the Atlantic Ocean for 18 August 1987. **b)** The map of TOMS reflectivity derived from 380 nm channel for 18 August 1987.

Plate 1b depicts the map of TOMS reflectivity measured at 380 nm on the same day. For comparison, the GOES-7 visible image at 1503 UTC, August 18, 1987, is shown in Figure 1. Both single-channel TOMS and GOES-7 maps show broken clouds in the northern South America continent and a bank of clouds extending from western Brazil into southern Argentina. Clouds were also clearly seen from the coastal region near Rio de Janeiro into the Atlantic Ocean. However, in the GOES-7 image, there were some plumes visible in Brazil that coincide with the location of the TOMS detected smoke plume depicted in Plate 1a, but were not observed in the TOMS 380 nm reflectivity map. It suggests that this GOES-7 "white" plume has different UV optical characteristics from the clouds and is mostly likely to be the smoke generated by the biomass burning in Brazil.

Seasonal Variation of Biomass Burning in 1988

In order to study the seasonal variation of biomass burning intensity in South America, TOMS R_{380} - R_{340} reflectivity difference values were averaged daily within a selected box between 0° and 20°S and 40°W - 70°W. Figure 2 shows the time series of these daily values in 1988. From the strong peak it is apparent that the tropospheric UV-absorbing aerosol level in South America is much higher in the dry season (August, September and early October), as compared to the rest of the year. This is consistent with the result of the seasonality of biomass burning fires reported by Setzer and Pereira [1991], based on a satellite survey in Amazonia, and with the seasonality of aerosol

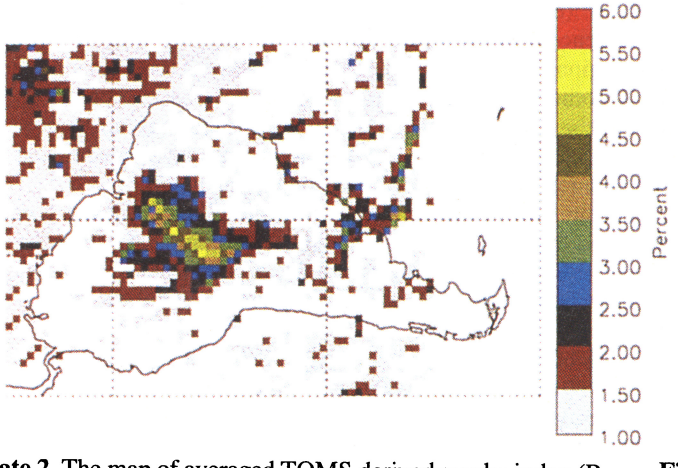

Plate 2. The map of averaged TOMS derived smoke index (R_{380}-R_{340}) over South America from August 25 to 30, 1992.

Figure 1. GOES-7 24-km resolution visible image at 1503 UTC for 18 August 1987.

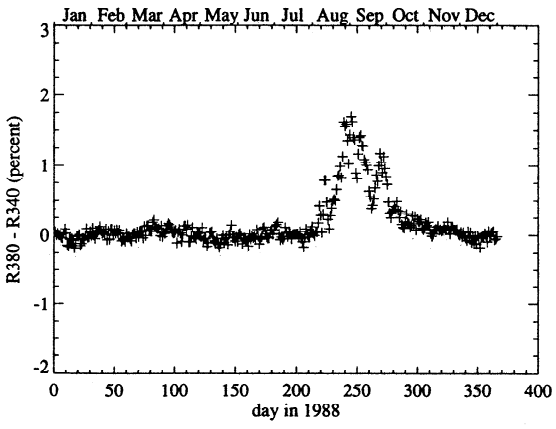

Figure 2. The seasonal variation of the TOMS derived smoke index (R_{380}-R_{340}) averaged daily over South America (0° - 20°S and 40°W - 70°W) for 1988.

optical depth in Cuiaba, Brazil measured by ground sunphotometer [Holben et al., 1995].

The statistics of the TOMS observed smoke covered areas over South America was also calcuclated for the period of August, September and October in 1988. Some smoke was found by TOMS in the region near Rio de Janeiro around the east coast of Brazil, which were probably due to the seasonal burning of agricultural stubble. However, a significant amount of smoke palls were detected by TOMS over the states of Rondonia, Mato Grosso, Goias, Tocantins, and Maranhao in Brazil. Most of the biomass burning fires in these regions are for the purpose of forest clearing and seasonal cerrado (savanna) burning, while some are due to agricultural burning [Malingreau and Tucker, 1988; Booth, 1989; Setzer and Pereira, 1989]. The haze aerosols generated in these regions were seen in TOMS data to be transported southward into Bolivia, Paraguay and northern Argentina by the prevailing winds. The TOMS estimated smoke covered areas are consistent with the results of the estimated areas of the deforestation and savanna clearing in different states of Brazil reported by Fearnside [1991].

Comparison With Ground-Based Measurements

There were only sporadic aerosol data available from ground-based instruments in South America, before the automatic sunphotometer network started to function in June 1993 [Holben et al., 1995]. Because Nimbus-7 TOMS ceased operation in May 1993, a limited ground data set obtained in the biomass burning season of 1992 was used to compare with the TOMS results. Figure 3 shows the aerosol optical thickness measurements at 441 nm wavelength obtained by a ground-based sunphotometer located at Porto Nacional, Brazil during September 12 - 20, 1992. For qualitative comparison, the TOMS overpass data of reflectivity difference within a 1°x1° window centered at Porto Nacional were also reported in Figure 3. Based upon the sunphotometer measurements, there is a strong diurnal variation in the intensity of the local burning at this site. The level of atmospheric aerosols started to build up near 11:00 local time and peaked at roughly 16:30 local time. These short-lived hazes mostly dissipated overnight before the burning started again late the next morning. Since the coincident TOMS measurements were taken at about 11:00 local time, low aerosol content was reported by TOMS during September 12 - 16 (day 256 - 260), except for day 259 due to a gap in TOMS measurements.

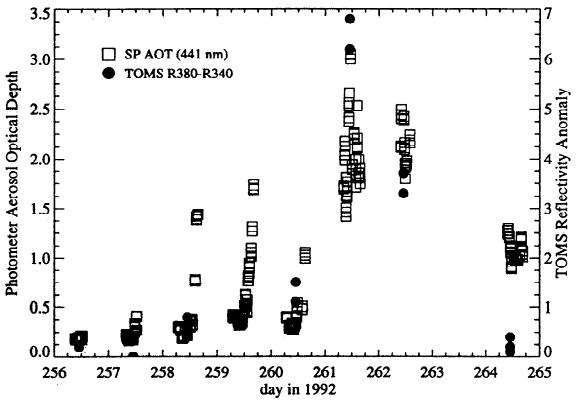

Figure 3. The comparison of the TOMS derived smoke index (R_{380}-R_{340}) with the sunphotometer measurements obtained at Porto Nacional, Brazil during September 12-20, 1992. The sunphotometer aerosol optical thickness (□) is measured at 441 nm and scaled on the left-hand side of the figure. The TOMS smoke index (•) is scaled on the right-hand side of the figure.

On September 17 and 18 (day 261 and 262), according to local ground-based reports, there were massive savanna burnings in the neighborhood of Porto Nacional. The intensive smoke plumes generated from these savanna fires were advected into the range of the measurement sensor by the prevailing wind. There were no ground measurement made on September 19 (day 263) because of the amount of cloudiness. By the end of the September 20 (day 264), some of the aged haze transported into the measurement location had disappeared. Despite the coarse spatial resolution of TOMS measurements (50 km at nadir and 115 km at far off nadir), the TOMS data gave generally consistent results with the sunphotometer measurements regarding measured smoke intensities and frequency of occurrence.

Transport of Aerosols

A 5-day forward trajectory calculation of air parcels was made with the Goddard model (Schoeberl et al., 1992), based upon archived ECMWF (European Centre for Medium-range Weather Forecasting) wind fields for August 25 - 30, 1992. These air

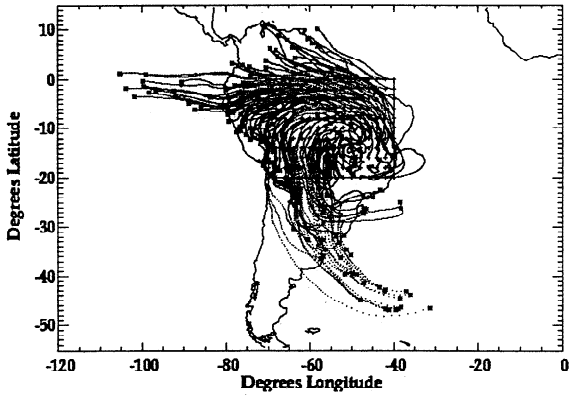

Figure 4. The output of a 5-day forward trajectory of air parcels on 310°K isentropic surface calculated by the Goddard model using ECMWF winds during August 25 - 30, 1992. The initial positions of the air parcels are labeled by (+), while the final locations are labeled by (*).

parcels were initiated on a 2°x2° grid points between 0° - 20°S and 40°W - 70°W and on the 310° K isentropic surface (~ 700 mb). Figure 4 shows that smoke generated in the region north of 5°S and west of 60°W tends to move to the west and to exit the continent into the Pacific Ocean near Ecuador. Smoke originating in the region south of 5°S are transported toward the Andes, get deflected southward, and exit the continent into the Atlantic Ocean near Buenos Aires and Sao Paulo.

This is consistent with the TOMS observed aerosol movements in the 5 day composite map for the same time period, as shown in Plate 2. Smoke particulates were observed over the states of Rondonia, Mato Grosso, and Para, Brazil, and extending southward over Argentina and Uruguay and over the Atlantic Ocean. Saharan desert dust was also visible in the equatorial Atlantic Ocean. These motions are confirmed in the movie studies of the TOMS reflectivity difference maps.

Conclusions

The reflectivity difference between TOMS 340 and 380 nm channels provides information about the global distribution of UV-absorbing soot aerosols, smoke, and desert mineral dust. The temporal and spatial variations of TOMS absorbing aerosol indices show good agreement with the results from ground-based measurements and satellite imagery. In addition, comparisons between single channel reflectivity and reflectivity difference data show that TOMS data can clearly distinguish between absorbing particles (smoke and dust) and non-absorbing aerosols (clouds and haze).

In the absence of information on particle size distributions and refractive indices to determine optical depths, the reflectivity difference can be used as a smoke index for the studies of biomass burning. TOMS data provide daily geographical distribution of the tropospheric absorbing aerosol indices which can be used as an input for model calculations of planetary radiative forcing. In addition, the observed movement of the smoke and aerosols could help validate models of calculated tropospheric circulation and air mass trajectories. TOMS daily global maps of the absorbing aerosol index can provide better interpretations of the production and loss of aerosol masses measured at the ground stations around the world. This suggests that TOMS reflectivity differences between 340 and 380 nm can serve as a global monitor for tropospheric absorbing aerosol, and for studies of the impact of biomass burning on the global climate change in terms of radiation, dynamics and photochemistry.

Acknowledgements. The authors would like to acknowledge the efforts of the TOMS Ozone Processing Team (OPT) for the new Version 7 data. We thank D. P. McNamara (Applied Research Corporation) for providing us with output from the Goddard trajectory model developed by M.Schoeberl, L. Lait, and P. Newman. The NOAA-NASA GOES Pathfinder program is also acknowledged for the GOES-7 visible imagery.

References

Booth, W., Monitoring the Fate of the Forests from Space, Science, 243, 1428-1429, 1989.

Connors, V.S., et al., Savanna Burning and Convective Mixing in South Africa: Implications for CO Emissions and Transport, The MIT Press, Cambridge, Massachusetts, 1991.

Cros, B., D. Nganga, R.A. Delmas, and J. Fontan, Tropospheric Ozone and Biomass Burning in Intertropical Africa, The MIT Press, Cambridge, Massachusetts, 1991.

Fearnside, P.M., Greenhouse Gas Contributions from Deforestation in Brazilian Amazonia, Global Biomass Burning: Atmospheric, Climatic and Biospheric Implication, The MIT Press, Cambridge, Massachusetts, 1991.

Haywood, J.M., and K.P. Shine, The Effect of Anthropogenic Sulfate and Soot Aerosol On The Clear Sky Planetary Radiation Budget, Geophy. Res. Lett., 22, 603-606, 1995.

Holben, B. N., et al., Multi-Band Automatic Sun and Sky Scanning Radiometer System For Measurement of Aerosols, Remote Sensing of Environ., to be published, 1995.

Kaufman, Y. J., et al., Biomass Burning Airborne and Spaceborne Experiment in the Amasonas (BASE-A), J. Geophys. Res., 97, 14,581-14,599, 1992.

Malingreau, J.P., and C.J. Tucker, Large-Scale Deforestation in the Southeastern Amazon Basin of Brazil, Ambio, 17, 49-55, 1988.

Matson, M., and B. Holben, Satellite Detection of Tropical Burning in Brazil, Int. J. Remote Sensing, 8, 509-516, 1987.

Prins, E.M., and W.P. Menzel, Geostationary Satellite Detection of Biomass Burning in South America, Int. J. Remote Sensing, 13, 2783-2799, 1992.

Robinson, Problems in Global Fire Evaluation: Is Remote Sensing the Solution, Global Biomass Burning: Atmospheric, Climatic and Biospheric Implication, The MIT Press, Cambridge, Massachusetts, 1991.

Robock, A., Surface Temperature Effects of Forest Fire Smoke Plumes, In Aerosol and Climate, A Deepak Publishing, Hampton, Virginia, 1988.

Schoeberl, M.R., L.R. Lait, P.A. Newman, and J.S. Rosenfield, The Structure of The Polar Vortex, J. Geophys. Res., 97, 7859-7882, 1992.

Setzer, A.W., and M.C. Pereira, Amazon Biomass Burnings in 1987 and Their Tropospheric Emissions, Ambio, 20, 19-20, 1991.

Westphal, D.L., O.B. Toon, and W.R. McKie, Atmospheric Effects of a Canadian Forest Fire Smoke Plume, IRS'88: Current Problems in Atmospheric Radiation, A Deepak Publishing, Hampton, Virginia, 1989.

P. K. Bhartia, J. F. Gleason, J. R. Herman and A. M. Thompson, Code 916, NASA/ Goddard Space Flight Center, MD 20771. (e-mail: herman@tparty.gsfc.nasa.gov)

B. N. Holben, Code 923, NASA/Goddard Space Flight Center, MD 20771.

T. F. Eck, N. C. Hsu and C. J. Seftor, Hughes STX, 7701 Greenbelt Rd, suite 400, Greenbelt, MD 20770. (e-mail: hsu@hoss.stx.com)

(Received October 13, 1995; accepted December 15, 1995)